EurJIC European Journal of Inorganic Chemistry

ChemPubSoc Europe

FULL PAPER

DOI:10.1002/ejic.201402412

Seleno-Nucleobases and Their Water-Soluble Ruthenium–Arene Half-Sandwich Complexes: Chemistry and Biological Activity

Raja Mitra,[a] Anup K. Pramanik,[a] and Ashoka G. Samuelson*[a]

Keywords: Bioorganic chemistry / Medicinal chemistry / Antitumor agents / Nucleobases / Half-sandwich complexes / Ruthenium / Selenium

Half-sandwich organometallic ruthenium complexes of seleno-nucleobases, **3** and **4**, were synthesized and characterized. The structures of both complexes were determined by X-ray crystallography and are the first crystal structures of ruthenium complexes with seleno-nucleobases. Interestingly, **3** self-assembles aided by adventitious water in DMF to give a tetranuclear square **3a**·6H_2O. Complex **4** is active against Jurkat and Molt-4 cell lines but inactive against the K562 cell line, whereas **3** is completely inactive against all three cell lines. The free ligand 6-selenopurine (**1**) and 6-selenoguanine (**2**) are highly active against these cell lines. Compound **2**, like its thio analogue, is unstable under UVA light, whereas **4** is stable under similar conditions, which suggests that the ruthenium complex could reduce problems associated with the instability of the free ligand, **2**, under irradiation.

Introduction

Derivatives of nucleobases have great potential for bioactivity. Therefore, it is not surprising that they have been extensively explored as therapeutic agents. In particular, 6-thioguanine (6-TG) has been used as an oral drug to treat different types of leukemia.[1] It has also been used as an immunosuppressant to treat patients with transplanted organs.[1] Its therapeutic value is drastically marred by side effects, which include skin cancer from exposure to ultraviolet A (UVA) light as a result of a photoreaction in which 6-TG is transformed to carcinogenic G^{SO3}.[2] In this context, it is interesting that antilymphoma activities of seleno derivatives of natural nucleobases have been explored since the 1960s.[3] However, the instability and toxicity of 6-selenopurine (**1**) and 6-selenoguanine (**2**) as aqueous solutions have restricted their clinical applications.[4]

One way of stabilizing a heterocyclic molecule is to coordinate it to a metal. Both **1** and **2** have been studied as Pt^{II} complexes by Kanzawa et al. (Figure 1).[5] Although [Pt(6-selenoguanine)$(NH_3)_2$] was found to be stable in aqueous media relative to [Pt(6-selenoguanine)$_2$], it decomposed rapidly in mouse serum to give the active component derived from cisplatin. However, the cytotoxicity of the [Pt(6-selenoguanine)$(NH_3)_2$] was significantly less than that of cisplatin or 6-selenoguanine.[6]

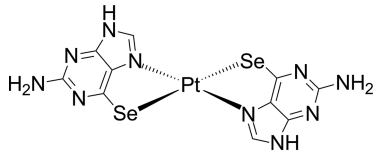

Pt(6-selenoguanine)$_2$

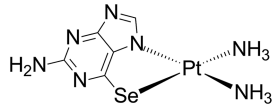

Pt(6-selenoguanine)$(NH_3)_2$

Figure 1. Structures of 6-selenoguanine-containing Pt^{II} complexes.

Side effects observed in platinum-based drugs are compelling scientists to look elsewhere for anticancer agents.[7] Ruthenium-based complexes are receiving extensive attention over other metal complexes owing to transferrin-based selective internalization into cancer cells.[8] In 2001, Sadler and co-workers showed that organometallic half-sandwich ruthenium complexes with ethylenediamine as an ancillary ligand are potentially anticancer active.[9] Since then many other organometallic ruthenium complexes with various ancillary ligands have been evaluated for anticancer[10] as well as antimetastatic activities.[11] In the last few years, many biologically active compounds have been used as ancillary ligands to synthesize anticancer active ruthenium half-sandwich complexes.[12] Multinuclear organometallic ruthenium complexes have also shown potential anticancer activity against cisplatin-resistant cell lines.[13] It is evident that tuning of ruthenium complexes can lead to better activity.[14]

[a] Department of Inorganic and Physical Chemistry, Indian Institute of Science, Bangalore 560012, India
E-mail: ashoka@ipc.iisc.ernet.in
http://ipc.iisc.ernet.in/~ashoka/

Supporting information for this article is available on the WWW under http://dx.doi.org/10.1002/ejic.201402412.

We report here the synthesis and characterization of two new ruthenium half-sandwich complexes, **3** and **4**, which bear 6-selenopurine (**1**) and 6-selenoguanine (**2**) as ancillary ligands, their reactivity, and their anticancer activity against three different leukemia cell lines. We have also explored the effects of UVA light on the stability of **2** and **4**.

Results and Discussion

Treatment of $[\{(\eta^6\text{-cymene})RuCl_2\}_2]$ with two equivalents of the seleno-nucleobase in dry dichloromethane resulted in the formation of the expected half-sandwich complex as a precipitate in reasonable yields (Scheme 1). All ligands and complexes were characterized by ^1H, $^{13}C\{^1H\}$, and ^{77}Se NMR spectroscopy, UV/Vis spectroscopy, HRMS, and elemental analysis.

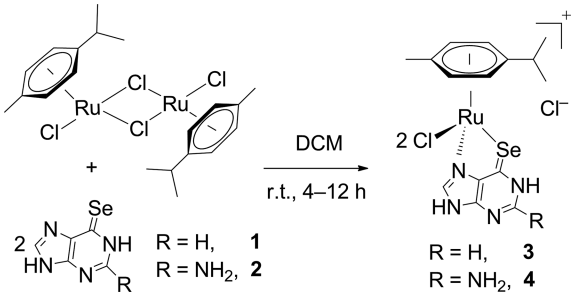

Scheme 1. Synthetic route used for the preparation of the complexes.

Resonances in the ^1H NMR spectra of the complexes were downfield-shifted (δ = 0.5 to 1 ppm) relative to the free ligand (Figure S1 in the Supporting Information). The ratio of the ligand to the cymene in the complex was as expected (1:1) on the basis of the ^1H NMR spectra. In the case of **4**, a peak at δ = 14.19 ppm in the ^1H NMR spectrum suggests the presence of a NH proton. However, the NH peak was absent in the case of **3**, which suggested further interactions of the ligand with another ruthenium center in DMSO. The presence of a multinuclear species was also indicated by the ^{13}C NMR spectrum of **3**, for which two sets of CH_3, CH, and cymene peaks were present. Such a doubling in the number of ^{13}C signals often arises from the presence of a multinuclear species (Figure S2). However, the ^{13}C NMR spectrum of **4** showed only fifteen resonances for carbon atoms, which suggested a mononuclear species. ^{77}Se NMR spectroscopy revealed that on coordination to Ru^{II} the ^{77}Se peaks due to **1** (δ = 375.5 ppm) and **2** (δ = 384.5 ppm) are upfield-shifted to δ = 368.3 and 349.1 ppm, respectively (Figure 2).

ESI-MS spectra of **3** and **4** in acetonitrile resulted in the removal of HCl and Cl^- from the complex. In the positive-ion mode, a singly charged species that corresponded to the ion $[(\eta^6\text{-cym})Ru(\text{seleno-nucleobase})\text{–}H]^+$ (cym = cymene) was observed at *m*/*z* 434.9658 and 449.9772 in the ESI-MS spectra for **3** and **4**, respectively (Figure S3 in the Supporting Information). Insignificant amounts of multinuclear ruthenium species (<2–5% of dinuclear species) were observed, which suggested that in acetonitrile solution both complexes stay in the mononuclear form. The formation and stabilization of multinuclear species, as discussed below, is dependent on the solvent.

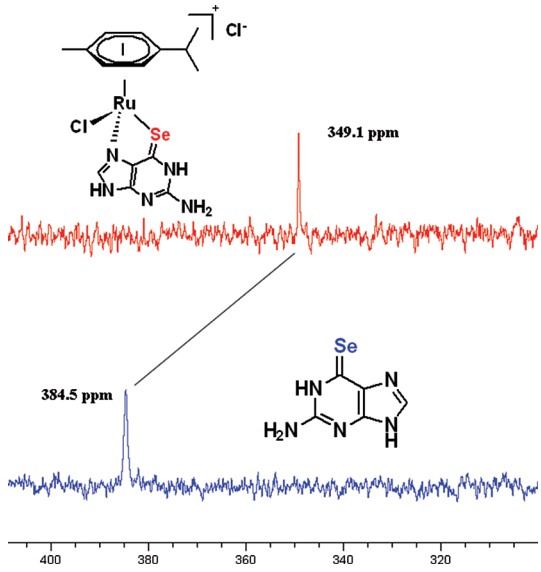

Figure 2. Comparison of ^{77}Se NMR for **2** and **4** in $[D_6]$DMSO.

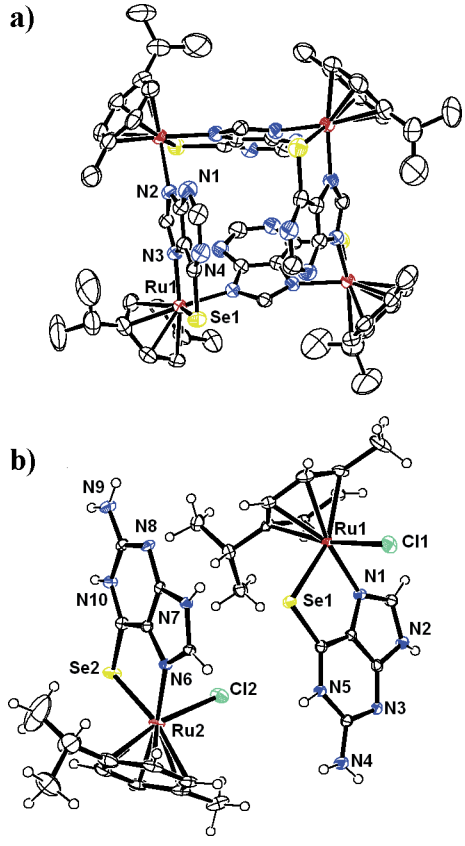

Figure 3. ORTEP view of (a) **3a**·6H_2O and (b) **4**·DMF·H_2O at 40% thermal ellipsoid. Solvents of crystallization and counteranions have been omitted for clarity. Hydrogen atoms have also been omitted in **3a**·6H_2O for clarity.

The molecular structures of **3** and **4** were determined by X-ray crystallography and appear to be the first examples of ruthenium complexes that contain seleno-nucleobases as ligands. Single crystals suitable for crystal structure analysis by X-ray diffraction were obtained in both cases by diffusing diethyl ether into a concentrated solution of the complex in DMF. In both complexes, Ru^{II} adopts the "three-legged piano-stool" pseudo-octahedral geometry. Complex **3** formed small needle-shaped crystals and was shown to be a mononuclear ruthenium complex on the basis of crystallographic analysis (Figure S4 in the Supporting Information). However, the data quality of this needle-shaped crystal was poor owing to its small size. Slow recrystallization from DMF/diethyl ether gave larger rectangular crystals, which were shown by X-ray crystallography to be a tetranuclear ruthenium complex **3a**·6H_2O (Figure 3). It is likely that mononuclear **3** as a solution in DMF undergoes substitution of chloride by adventitious water, present in the DMF, followed by the loss of H^+.[15] The deprotonated 6-selenopurine ligand replaces the water in an intermolecular substitution to form a square tetranuclear species, which crystallizes to give **3a**·6H_2O (Scheme 2).

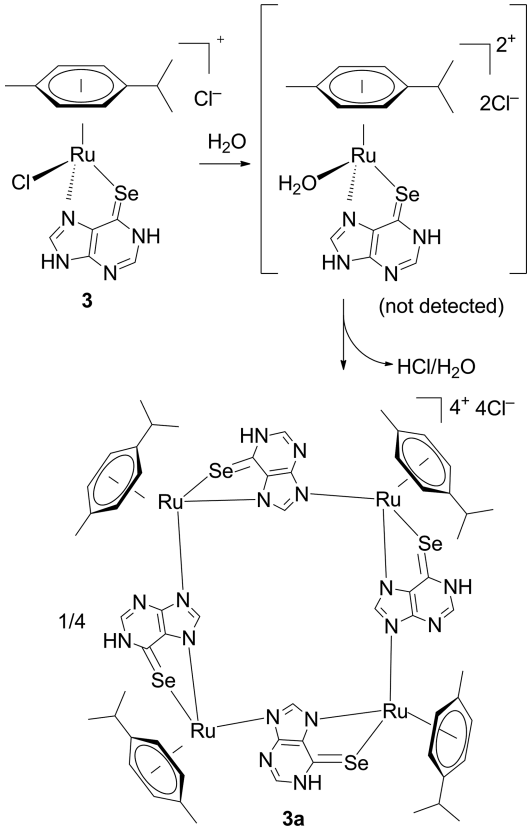

Scheme 2. Formation of tetranuclear **3a** from mononuclear **3**.

Complex **4** showed a mononuclear structure with chloride as the counteranion (**4**·DMF·H_2O) (Figure 3). The extra amine group present in **2** clearly has a role to play in preventing the formation of tetranuclear species in the case of **4**. Key bond lengths are given in Table 1, and crystallographic parameters are given in the Supporting Information (Table S1).

Table 1. Selective bond lengths [Å] and angles [°] for **3a**·6H_2O and **4**·DMF·H_2O.

3a·6H_2O		**4**·DMF·H_2O	
Ru1–Se1	2.5574(9)	Ru1–Se1	2.5337(8)
		Ru2–Se2	2.5486(11)
Ru1–N2	2.107(5)	Ru1–Cl1	2.3994(13)
		Ru2–Cl2	2.3956(14)
Ru1–N3	2.095(5)	Ru1–N1	2.102(3)
		Ru2–N6	2.109(3)
N2–Ru1–N3	81.80(18)	N1–Ru1–Cl1	83.13(10)
		N6–Ru2–Cl2	83.55(10)
N2–Ru1–Se1	89.07(14)	N1–Ru1–Se1	84.50(7)
		N6–Ru2–Se2	84.13(9)
Se1–Ru1–N3	84.35(13)	Se1–Ru1–Cl1	86.67(4)
		Se2–Ru2–Cl2	86.89(4)

In all complexes, Ru1–Se1 distances range from 2.5337(8) to 2.5574(9) Å and are longer than the previously reported ruthenium complexes bearing a Ru–Se bond [2.497(5) Å].[16] The double-bond character of the C=Se unit is retained as the distances are found to be 1.868(6) and 1.837(4) Å for **3a**·6H_2O and **4**·DMF·H_2O, respectively. The complexes are capable of extensive intermolecular hydrogen bonding, which is reflected in the crystal structures (Figure S5 in the Supporting Information).

Lipophilicity

It was very interesting to observe the contrasting solubility behavior of the ligands and their ruthenium complexes. As the lipophilicity of a compound is an important parameter in determining its biodistribution, this contrasting behavior suggests a way by which the complex can reach a site inaccessible to the ligand. Therefore the lipophilicity (log *P*) of the complexes was measured using UV/Vis spectroscopy. Aqueous solutions of all complexes were partitioned independently with *n*-octanol for 4 h at 37 °C. Concentrations of the complex in the aqueous phase before and after partitioning with *n*-octanol were measured. Both complexes have a negative log *P* value, -0.98 ± 0.12 and -0.75 ± 0.27, respectively, for **3** and **4**, which is consistent with their high water-solubility.

Solution Chemistry

The stability of the metal complexes in aqueous media plays an important role in biological activity. The stability of both complexes was monitored by UV/Vis and ^{1}H NMR spectroscopy. The complex was dissolved in dry methanol and was diluted further with water (95% v/v). A change in absorbance with respect to time was monitored using UV/Vis spectroscopy. Both complexes showed small changes in the UV/Vis spectra with time (Figure S6 in the Supporting Information).

^{1}H NMR spectra were recorded in D_2O. Both complexes showed no changes over short reaction times. Whereas complex **4** showed no change even after 24 h, complex **3** indicated the formation of a new species, which presumably cor-

responded to the tetranuclear species. Diffusion-ordered spectroscopy (DOSY) experiments suggest that complex **4** has a hydrodynamic radius of 5.16 Å consistent with a monomeric structure. DOSY data could not be obtained from complex **3** immediately after dissolving in D_2O as the intensity of the peaks slowly changed with time. After incubation for seven days, the presence of monomeric and tetrameric species with the corresponding hydrodynamic radii of 5.26 and 7.83 Å could be inferred. NMR spectra and DOSY data are given in the Supporting Information (Figure S7).

To gain insight into the nature of molecular structures in aqueous solution, high-resolution ESI-MS studies were carried out with solutions of **3** and **4**. Peaks that correspond to [(η^6-cym)RuSeNBX] or [(η^6-cym)RuSeNB(OH_2)]$^+$ (NB = nucleobase) were not observed for any of the complexes, which suggests a weak Ru–X/O bond that readily dissociates under the ESI-MS conditions. Complex **3** showed peaks that correspond to a mononuclear species (*m*/*z* 434.9669) and a dinuclear ruthenium species (*m*/*z* 866.9276) with equal relative intensities (Table 2). Peaks that correspond to a trinuclear (*m*/*z* 1297.8807) and a tetranuclear (*m*/*z* 1730.8606) species were also observed in ESI-MS spectra with a relative abundance around 5%. Isotopic distribution of all peaks matched exactly with the expected natural abundance values. A representative comparison between theoretical and experimental isotopic distribution is shown in Figure 4. Complex **4** shows two peaks that correspond to a mononuclear (*m*/*z* 449.9776) and a dinuclear (*m*/*z* 897.0039) species (Figure S8 in the Supporting Information). No trinuclear and tetranuclear ruthenium species were observed.

Table 2. Values of *m*/*z* of Ru complexes in aqueous solution obtained in ESI-MS.

	Observed peak $[M]^+$	Empiriical formula (calcd. *m*/*z*)	Found *m*/*z*
3	[(η^6-cym)Ru(**1**-H)]$^+$	$[C_{15}H_{17}N_4SeRu]^+$ (434.9670)	434.9669
	[{(η^6-cym)Ru(**1**-H)}$_2$ + H]$^+$	$[C_{30}H_{33}N_8Se_2Ru_2]^+$ (866.9270)	866.9276
	[{(η^6-cym)Ru(**1**-H)}$_3$ + H]$^+$	$[C_{45}H_{49}N_{12}Se_3Ru_3]^+$ (1298.8880)	1298.8837
	[{(η^6-cym)Ru(**1**-H)}$_4$ + H]$^+$	$[C_{60}H_{65}N_{16}Se_4Ru_4]^+$ (1730.8490)	1730.8606
4	[(η^6-cym)Ru(**2**-H)]$^+$	$[C_{15}H_{18}N_5SeRu]^+$ (449.9779)	449.9776
	[{(η^6-cym)Ru(**2**-H)}$_2$ + H]$^+$	$[C_{30}H_{35}N_{10}Se_2Ru_2]^+$ (896.9490)	897.0039

In contrast to the aqueous solutions, solutions of both complexes in acetonitrile show mononuclear species as the major peak in the ESI-MS spectra. It suggests that water plays an important role in the formation of multinuclear species. As the synthesis of complexes is carried out in dry CH_2Cl_2, under an inert atmosphere, it is likely that the complexes are formed as mononuclear species.

We propose that **3** attains a stable tetranuclear structure aided by water in DMF as seen from the X-ray structure determination. This is also consistent with the ^{1}H NMR spectroscopic splitting patterns recorded in DMSO that contained water. However, under the ESI-MS conditions, it becomes fragmented, thereby resulting in the formation of mononuclear, dinuclear, and trinuclear ruthenium species. Complex **4** stays mostly in the mononuclear form with a small amount of the dinuclear ruthenium species (Table S2 in the Supporting Information) as observed in the ESI-MS spectrum.

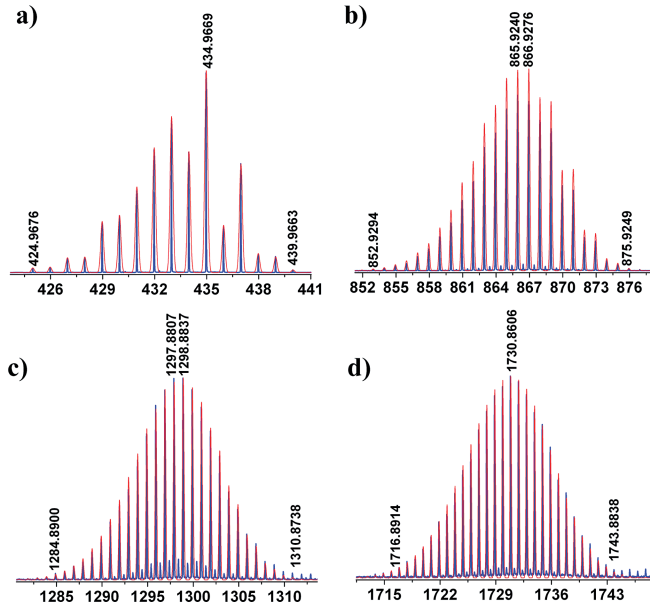

Figure 4. Theoretical (red) and observed (blue) isotopic distribution of (a) mononuclear, (b) dinuclear, (c) trinuclear, and (d) tetranuclear ruthenium species observed in the HR ESI-MS spectra of **3** in water.

Growth Inhibition by Sulforhodamine B (SRB) Assay

We have recently identified ruthenium complexes of 6-TG that are anticancer-active against several leukemia cell lines.[17] It would be interesting to see if the selenium analogue of 6-TG and their corresponding ruthenium complexes can also exhibit antileukemic activity. Growth inhibition (GI_{50}) of ligands and their corresponding ruthenium complexes were checked against K562 (chronic myelogenous leukemia), Jurkat (leukemic T cell lymphoblast), and Molt-4 (leukemic T cell lymphoblast) cell lines by means of the sulforhodamine B assay.[18] The results are listed in Table 3, and the experimental details are given in the Supporting Information. Both ligands were found to be active against K562 and Jurkat cell lines. However, against the Molt-4 cell line only **2** was found to be active (<0.1 μM) relative to **1** (15.6 μM). Surprisingly, complex **3** was inactive against all the leukemia cell lines we tested including those cell lines for which ligand **1** is active (K562 and Jurkat). Interestingly, **4** was active against Jurkat and Molt-4 cell lines, whereas against the K562 cell line it is completely inactive (58.5 μM).

Table 3. In vitro growth inhibition of human cancer cell lines after exposure to ligands or [(η^6-cymene)Ru^{II}Cl(seleno-nucleobases)] complexes for 48 h.

	GI_{50} [μM]		
Compound	K562 (chronic myelogenous leukemia)	Jurkat (leukemic T cell lymphoblast)	Molt-4 (leukemic T cell lymphoblast)
1	<0.1	<0.1	15.6
2	<0.1	<0.1	<0.1
3	79.9	54.2	53.4
4	58.5	<0.1	7.4
Adriamycin	<0.1	<0.1	<0.1

Photochemistry

Despite the comparable anticancer activity of **2** with 6-TG, extensive studies with the former have not been carried out as it offers no advantages over 6-TG.[4b] We have recently shown that the ruthenium half-sandwich framework stabilizes 6-TG against UVA light.[17b] We wished to check to see if **2** and **4** suffered from any of the problems reported in the case of 6-TG in the presence of UVA light in aqueous solutions. UV/Vis spectra before and after photoirradiation (10 and 30 min) suggest that **2** is unstable under UVA irradiation. A decrease in the 360 nm band was observed with an increase in the 317 nm band (Figure 5). Photoirradiation also caused an increase in the fluorescence at 390 nm (λ_{em}) when excited at 317 nm (λ_{ex}) (Figure S10 in the Supporting Information). However, **4** was found to be quite stable (Figure 5) under similar conditions. Although **4** is less potent than **2**, it is possible that the photostability of **4** would be an advantage during long-term usage and in its selective delivery through transferrin.

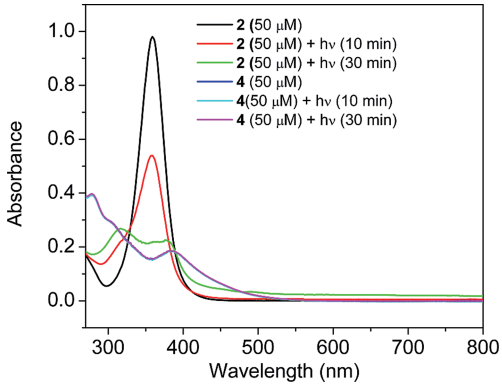

Figure 5. UV/Vis spectra of **2** and **4** in aqueous solution containing 1% DMSO before and after irradiation (10 and 30 min) with UVA light.

Conclusion

We have successfully synthesized and characterized the first bioorganometallic half-sandwich ruthenium complexes of seleno-nucleobases. Of the two water-soluble complexes **3** and **4**, only **4** is active. Although complex **3** retains the ratio of seleno-nucleobase to cymene, on the basis of the MS analysis, it is inactive and is shown to be a tetranuclear species on the basis of DOSY-NMR spectroscopy and crystallography. Anticancer activities of seleno-nucleobases are reduced upon coordination to the ruthenium center. Although **4** showed less cytotoxicity, its stability in aqueous media under UVA light makes it worthy of further study as an alternative to the unstable **2**. Further studies are underway to confirm the potential application of these ruthenium complexes as anticancer agents.

Experimental Section

Materials and Methods: $RuCl_3 \cdot xH_2O$ and selenourea were obtained from Sigma–Aldrich (India). α-Phellandrene was purchased from Merck, India. 6-Chloropurine and 6-chloroguanine were purchased from SRL, India. Precursors for ruthenium complexes were prepared according to the literature procedures.[19] All reactions were carried out in an atmosphere of dry nitrogen using standard Schlenk and vacuum-line techniques, and the solvents were dried by standard methods.[20] ^1H, $^{13}C\{H\}$, and ^{77}Se NMR spectra were recorded with a Bruker AMX 400 NMR spectrometer operating at 400 MHz for ^1H, 100 MHz for ^{13}C, and 76.3 MHz for ^{77}Se in [D_6]-DMSO or D_2O. Elemental analyses were performed with a Thermo Scientific Flash EA 1200 CHNS analyzer. HRMS of all samples were recorded with an Agilent 6538 Ultra-High Definition (UHD) Accurate-Mass Q-TOF. UV/Vis and fluorescence spectra were recorded with a Perkin–Elmer Lamda 35 UV/visible spectrophotometer and a Perkin–Elmer Lamda 50B spectrofluorometer, respectively. Growth inhibition (GI_{50}) by sulforhodamine B (SRB) assays were carried out by the Advanced Centre for Treatment, Research, and Education in Cancer (ACTREC), Mumbai, by following the literature procedure.[18]

Synthesis and Characterization

6-Selenopurine (1): 6-Selenopurine was synthesized according to the literature procedure.[3a] Yield 219 mg (56%, from 171 mg of 6-chloropurine). ^1H NMR (400 MHz, [D_6]DMSO, 20 °C): δ = 8.25 (d, J = 2.4 Hz, 1 H, C*H*), 8.54 (s, 1 H, C*H*), 13.8 (br. s, 1 H, N*H*), 14.27 ppm (br. s, 1 H, N*H*) ppm. ^{77}Se (76 MHz, [D_6]DMSO, 20 °C): δ = 375.5 ppm. $C_5H_4N_4Se \cdot H_2O$: calcd. C 27.66, H 2.79, N 25.81; found C 27.56, H 3.23, N 25.06. Q-TOF HRMS (CH_3CN): calcd. for $C_5H_5N_4Se^+$: 200.9675 [M + H^+], found 200.9674 (100%); calcd. 222.9493 [M + Na^+], found 222.9499 (19%).

6-Selenoguanine (2): 6-Selenogunaine was synthesized by adopting the procedure used for 6-selenopurine preparation. Briefly, 6-chloroguanine (200 mg, 1.18 mmol) and selenourea (148 mg, 1.2 mmol) were dissolved in ethanol (5 mL). The orange solution was heated under reflux conditions for 2 h to obtain an orange-yellow precipitate. The precipitate was filtered, washed with water, and dried in air. On the basis of thermogravimetric analysis (TGA) data, it was observed that three molecules of water were present, yield 320 mg (quantitative, considering three molecules of water). ^1H NMR (400 MHz, [D_6]DMSO, 20 °C): δ = 7.12 (br. s, 2 H, NH_2), 8.70 ppm (s, 1 H, C*H*) ppm. ^{13}C NMR (100 MHz, [D_6]DMSO, 20 °C): δ = 126.2, 143.3, 149.7, 155.2, 168.7 ppm. ^{77}Se (76 MHz, [D_6]DMSO, 20 °C): δ = 384.5 ppm. $C_5H_5N_5Se \cdot 2H_2O \cdot 0.2C_2H_5OH$: calcd. C 24.90, H 3.95, N 26.91; found C 25.11, H 3.21, N 27.07. Q-TOF HRMS (CH_3CN): calcd. for $C_5H_6N_5Se^+$: 215.9784 [M + H^+], found 215.9783 (100%); calcd. 237.9602 [M + Na^+], found 237.9606 (23%).

[Ru(η⁶-cymene)Cl(6-selenopurine)]Cl (3): 6-Selenopurine (48 mg, 0.24 mmol) was added to a solution of [{(η⁶-cymene)$RuCl_2$}$_2$] (75 mg, 0.12 mmol) in dry CH_2Cl_2 (5 mL). Within 30 min of stirring at room temperature, an orange-yellow precipitate was formed. The heterogeneous mixture was stirred for another 4.5 h. After that, it was filtered, washed with CH_2Cl_2 and then with diethyl ether, and dried in air to obtain a free-flowing bright orange-yellow powder, yield 72 mg (58%). ^{1}H NMR (400 MHz, [D$_6$]DMSO, 20 °C): δ = 1.08 [dd, J = 22.8, J = 6.8 Hz, 6 H, (CH_3)$_2$CH], 2.10 (s, 3 H, CH_3), 2.68 [sept, 1 H, (CH_3)$_2$CH], 5.72 (d, J = 5.6 Hz, 1 H, H–Ar$_{cymene}$), 5.94 (m, 2 H, H–Ar$_{cymene}$), 6.07 (d, J = 6.0 Hz, 1 H, H–Ar$_{cymene}$), 8.70 (s, 1 H, CH_{ligand}), 9.63 ppm (s, 1 H, CH_{ligand}) ppm. ^{13}C NMR (100 MHz, [D$_6$]DMSO, 20 °C): δ = 18.8, 19.3, 22.4, 22.6, 23.2, 30.9, 31.5, 81.3, 82.1, 83.0, 83.6, 86.4, 87.3, 100.5, 101.0, 103.6, 107.4, 139.9, 144.9, 148.8, 150.2, 167.8 ppm. ^{77}Se (76 MHz, [D$_6$]DMSO, 20 °C): δ = 369.5 ppm. UV/Vis (MeOH): λ_{max} (ε) = 358 (6100 $M^{-1}cm^{-1}$) nm; elemental analysis calcd. (%) for $C_{15}H_{18}N_4RuSeCl_2{\cdot}H_2O$: calcd. C 34.43, H 3.85, N 10.71; found C 34.16, H 3.98, N 10.12. Q-TOF HRMS (CH_3CN): calcd. for $C_{15}H_{17}N_4RuSe^+$: 434.9658 [M – 2Cl$^-$ – H$^+$]$^+$; found 434.9670.

[Ru(η⁶-cymene)Cl(6-selenoguanine)]Cl (4): 6-Selenoguanine·3H_2O (65 mg, 0.24 mmol) was added to a solution of [{(η⁶-cymene)$RuCl_2$}$_2$] (75 mg, 0.12 mmol) in dry CH_2Cl_2 (5 mL). Within 2 h of stirring at room temperature, an orange-yellow precipitate was formed. The heterogeneous mixture was stirred for another 12 h. After that, it was filtered, washed with CH_2Cl_2 and then with diethyl ether, and dried in air to obtain a free-flowing bright yellow powder. A needle-shaped single crystal suitable for X-ray diffraction was obtained from diffusion of diethyl ether into a solution of the complex in DMF, yield 96 mg (75%). ^{1}H NMR (400 MHz, [D$_6$]-DMSO, 20 °C): δ = 1.10 [dd, J = 18.4, J = 7.2 Hz, 6 H, (CH_3)$_2$-CH], 2.11 (s, 3 H, CH_3), 2.65 [sept, 1 H, (CH_3)$_2$CH], 5.66 (d, J = 6.0 Hz, 1 H, H–Ar$_{cymene}$), 5.80 (dd, J = 10.8, J = 6.0 Hz, 2 H, H–Ar$_{cymene}$), 6.01 (d, J = 6.0 Hz, 1 H, H–Ar$_{cymene}$), 7.72 (br. s, 2 H, NH_2), 9.19 (s, 1 H, CH_{ligand}), 14.12 ppm (br. s, 1 H, NH) ppm. ^{13}C NMR (100 MHz, [D$_6$]DMSO, 20 °C): δ = 19.3, 22.6, 23.1, 31.5, 81.0, 82.2, 82.9, 83.4, 100.5, 103.2, 133.5, 146.6, 147.9, 157.4, 165.3 ppm. ^{77}Se (76 MHz, [D$_6$]DMSO, 20 °C): δ = 349.1 ppm. UV/Vis (MeOH): λ_{max} (ε) = 378 (6600 $M^{-1}cm^{-1}$) nm. $C_{15}H_{19}N_5RuSeCl_2{\cdot}H_2O$: calcd. C 33.47, H 3.93, N 13.01; found C 34.17, H 3.95, N 12.70. Q-TOF HRMS (CH_3CN): calcd. for $C_{15}H_{18}N_5RuSe^+$: 449.9772 [M – 2Cl$^-$ – H$^+$]$^+$; found 449.9780.

Single-Crystal X-ray Crystallography: Single crystals of the complexes were separately mounted on a loop in Paratone oil along the largest dimension. Data were collected with a Bruker AXS single-crystal diffractometer controlled by the SMART (Version 5.05; Madison, WI, 1998) software package with a D8 Quest CMOS photon detector and a sealed Mo-K_α (λ = 0.71073) source working at 2.2 kW and 50/35 [kV/mA]. Intensity data were collected at room temperature for **3**, **3a**·6H_2O, and at 100 K for **4**·DMF·H_2O. Crystallographic computations were performed using the WinGX (1.63.02) package.[21] The data were corrected for Lorentz and polarization effects. The structures were solved by direct methods (using the module SIR-92) followed by the full-matrix least square procedure of F^2 for all reflections (SHELXL-97).[22] All non-hydrogen atoms were refined by anisotropic displacement parameters and hydrogen atoms were located or fixed at idealized positions. Structures were drawn using ORTEP-3.[23]

Lipophilicity (log *P*) Measurements: The lipophilicity of the complexes was measured by the standard "shake flask technique".[24] Experiments were carried out at (37 ± 1) °C in triplicate. Approximately 3 mg (1 mg mL^{-1}) of each of the complexes was dissolved in MilliQ water (3 mL). The stock solution was divided into two parts (1 and 2 mL) in glass vials. One part of the solution (1 mL) was taken and the absorbance recorded to obtain the value of A_0 after incubating at 37 °C for 4 h. Octanol was added (2 mL) to another part of the solution and stirred at 37 °C for 4 h. The water layer was separated and the absorbance was recorded to obtain A_0 – A ($A_{octanol}$). Values of log P were calculated using the following equation.

$$\log P = \log\left[\frac{A_{octanol}}{A_{water}}\right] = \log\left[\frac{A_0 - A}{A_0}\right] = \log\left[\frac{[Ru]_{oct}}{[Ru]_{water}}\right]$$

Solution Chemistry: Ruthenium complexes were dissolved in dry methanol to make a stock solution with a concentration of 1 mM. From this stock solution, 50 μL was added to water (950 μL) in a 1 mL cuvette to obtain a final concentration of 50 μM of the complex in 5% MeOH/water. The change in the absorption spectra was monitored by UV/Vis spectroscopy.

To monitor the hydrolysis by ^{1}H NMR spectroscopy, the complex was taken in a NMR spectroscopy tube. After dissolving the complex in D_2O, the ^{1}H NMR spectrum was recorded immediately and after 24 h. ^{1}H DOSY data was acquired with the standard Bruker ledbpgp2s program using 32 t_1 increments of 32 transients. The acquisition time was 1 s and the relaxation delay was 1.5 s (D1). The diffusion time was between 0.11 and 0.125 s (D_2O) and the rectangular gradient pulse duration was between 1.2 and 1.4 ms (P30). Gradient recovery delays of 200 μs followed the application of each gradient pulse. Data was accumulated by linearly varying the diffusion encoding gradients over a range from 5 to 95 % for 32 gradient increment values.

To detect the actual hydrolyzed products of ruthenium complexes, they were dissolved in LC-MS grade water to obtain a concentration of 2 mM. From this stock solution, 10 μL was added to MilliQ water (990 μL). This solution was infused into the ESI-MS instrument using an auto-injection module (Agilent 1290 infinity) attached to the ESI-MS [Agilent 6538 Ultra-High Definition (UHD) Accurate-Mass Q-TOF]. The same solution was infused after incubation at 298 K for 6 and 24 h. Mobile phase: 50% acetonitrile (LC-MS grade, Fluka)/50% water (purified using a Millipore system) that contained 0.1% formic acid (LC-MS grade, Agilent) with a flow rate of 0.3 mL min^{-1}. The capillary voltage and the fragmentor voltage were kept at 4.0 kV and 200 V, respectively. The capillary temperature was 350 °C with a 10 L h^{-1} flow of nitrogen drying gas. ESI-MS data were processed using the MassHunter software.

Photochemistry: Standard ferrioxalate actinometry was performed to standardize the UV radiation of the home-built photoreactor.[17b,25] The ruthenium complexes **4** and **2** (0.1 mM concentration in 8 mL of MilliQ water that contained 1% DMSO) were irradiated in a round-bottomed flask with continuous stirring. An aliquot (2 mL) was taken out after 10 min [(7 ± 1) kJ m^{-2}] and 30 min [(20 ± 1) kJ m^{-2}]. After irradiation, UV/Vis and fluorescence spectra of the solution were recorded.

CCDC-1000363 (for **3a**·6H_2O), -967546 (for **4**·DMF·H_2O), and -1000364 (for **3**) contain the supplementary crystallographic data for this paper. These data can be obtained free of charge from The Cambridge Crystallographic Data Centre via www.ccdc.cam.ac.uk/data_request/cif.

Supporting Information (see footnote on the first page of this article): Contains ^{1}H, ^{77}Se, ^{13}C NMR and high-resolution ESI-MS

spectra of all complexes, crystal structure of mononuclear complex **3**, crystallographic data and refinement parameters, various weak interactions in crystal, ^{1}H NMR spectra, UV/Vis and ESI-MS data of aqueous solutions for all complexes, and fluorescence spectra of **2** and **4** before and after photoirradiation.

Acknowledgments

The authors would like to thank the Department of Science and Technology (DST), New Delhi, for generous funding. R. M. thanks the Council of Scientific and Industrial Research (CSIR), New Delhi, for a Senior Research Fellowship. The authors would like to thank Dr. A. Juvekar of the Advanced Centre for Treatment, Research, and Education in Cancer (ACTREC), Mumbai, for growth inhibition data. The authors thank an anonymous referee for suggesting the DOSY experiment.

[1] P. Karran, N. Attard, *Nat. Rev. Cancer* **2008**, *8*, 24–36.
[2] a) P. O'Donovan, C. M. Perrett, X. Zhang, B. Montaner, Y.-Z. Xu, C. A. Harwood, J. M. McGregor, S. L. Walker, F. Hanaoka, P. Karran, *Science* **2005**, *309*, 1871–1874; b) X. Ren, F. Li, G. Jeffs, X. Zhang, Y.-Z. Xu, P. Karran, *Nucleic Acids Res.* **2010**, *38*, 1832–1840.
[3] a) H. G. Mautner, *J. Am. Chem. Soc.* **1956**, *78*, 5292–5294; b) H. G. Mautner, J. J. Jaffe, *Cancer Res.* **1958**, *18*, 294–298; c) S.-H. Chu, *J. Med. Chem.* **1971**, *14*, 254–255.
[4] a) A. J. Repta, Y. A. Beltagy, *J. Pharm. Sci.* **1981**, *70*, 634–637; b) G. Mugesh, W.-W. du Mont, H. Sies, *Chem. Rev.* **2001**, *101*, 2125–2180.
[5] F. Kanzawa, M. Maeda, T. Sasaki, A. Hoshi, K. Kuretani, *J. Natl. Cancer Inst.* **1982**, *68*, 287–291.
[6] M. Maeda, N. Abiko, T. Sasaki, *J. Pharmacobio-Dyn.* **1982**, *5*, 81–87.
[7] a) S. H. van Rijt, P. J. Sadler, *Drug Discovery Today* **2009**, *14*, 1089–1097; b) D. Esteban-Fernández, J. M. Verdaguer, R. Ramírez-Camacho, M. A. Palacios, M. M. Gómez-Gómez, *J. Anal. Toxicol.* **2008**, *32*, 140–146; c) A. Bergamo, C. Gaiddon, J. H. Schellens, J. H. Beijnen, G. Sava, *J. Inorg. Biochem.* **2012**, *106*, 90–99; d) I. Romero-Canelón, P. J. Sadler, *Inorg. Chem.* **2013**, *52*, 12276–12291; e) N. P. E. Barry, P. J. Sadler, *Chem. Commun.* **2013**, *49*, 5106–5131; f) P. J. Dyson, G. Sava, *Dalton Trans.* **2006**, 1929–1933; g) K. D. Mjos, C. Orvig, *Chem. Rev.* **2014**, *114*, 4540–4563.
[8] a) M. Pongratz, P. Schluga, M. A. Jakupec, V. B. Arion, C. G. Hartinger, G. Allmaier, B. K. Keppler, *J. Anal. At. Spectrom.* **2004**, *19*, 46–51; b) L. Messori, F. Kratz, E. Alessio, *Met.-Based Drugs* **1996**, *3*, 1–9; c) W. Guo, W. Zheng, Q. Luo, X. Li, Y. Zhao, S. Xiong, F. Wang, *Inorg. Chem.* **2013**, *52*, 5328–5338; d) A. Martínez, J. Suárez, T. Shand, R. S. Magliozzo, R. A. Sánchez-Delgado, *J. Inorg. Biochem.* **2011**, *105*, 39–45; e) M. Klajner, C. Licona, L. Fetzer, P. Hebraud, G. Mellitzer, M. Pfeffer, S. Harlepp, C. Gaiddon, *Inorg. Chem.* **2014**, *53*, 5150–5158.
[9] a) R. E. Morris, R. E. Aird, P. del Socorro Murdoch, H. Chen, J. Cummings, N. D. Hughes, S. Parsons, A. Parkin, G. Boyd, D. I. Jodrell, P. J. Sadler, *J. Med. Chem.* **2001**, *44*, 3616–3621; b) R. E. Aird, J. Cummings, A. A. Ritchie, M. Muir, R. E. Morris, H. Chen, P. J. Sadler, D. I. Jodrell, *Br. J. Cancer* **2002**, *86*, 1652–1657; c) A. F. A. Peacock, P. J. Sadler, *Chem. Asian J.* **2008**, *3*, 1890–1899.
[10] a) G. Gasser, I. Ott, N. Metzler-Nolte, *J. Med. Chem.* **2011**, *54*, 3–25; b) C. G. Hartinger, P. J. Dyson, *Chem. Soc. Rev.* **2009**, *38*, 391–401; c) M. Patra, T. Joshi, V. Pierroz, K. Ingram, M. Kaiser, S. Ferrari, B. Spingler, J. Keiser, G. Gasser, *Chem. Eur. J.* **2013**, *19*, 14768–14772; d) R. Mitra, S. Das, S. V. Shinde, S. Sinha, K. Somasundaram, A. G. Samuelson, *Chem. Eur. J.* **2012**, *18*, 12278–12291; e) S. Das, S. Sinha, R. Britto, K. Somasundaram, A. G. Samuelson, *J. Inorg. Biochem.* **2010**, *104*, 93–104; f) C. M. Clavel, E. Păunescu, P. Nowak-Sliwinska, A. W. Griffioen, R. Scopelliti, P. J. Dyson, *J. Med. Chem.* **2014**, *57*, 3546–3558; g) F. Caruso, E. Monti, J. Matthews, M. Rossi, M. B. Gariboldi, C. Pettinari, R. Pettinari, F. Marchetti, *Inorg. Chem.* **2014**, *53*, 3668–3677; h) R. Mitra, A. G. Samuelson, *Eur. J. Inorg. Chem.* **2014**, 3536–3546.
[11] a) C. Scolaro, A. Bergamo, L. Brescacin, R. Delfino, M. Cocchietto, G. Laurenczy, T. J. Geldbach, G. Sava, P. J. Dyson, *J. Med. Chem.* **2005**, *48*, 4161–4171; b) C. S. Allardyce, P. J. Dyson, D. J. Ellis, S. L. Heath, *Chem. Commun.* **2001**, 1396–1397.
[12] a) A. Castonguay, C. Doucet, M. Juhas, D. Maysinger, *J. Med. Chem.* **2012**, *55*, 8799–8806; b) A. Kurzwernhart, W. Kandioller, E. A. Enyedy, M. Novak, M. A. Jakupec, B. K. Keppler, C. G. Hartinger, *Dalton Trans.* **2013**, *42*, 6193–6202; c) W. Kandioller, E. Balsano, S. M. Meier, U. Jungwirth, S. Goschl, A. Roller, M. A. Jakupec, W. Berger, B. K. Keppler, C. G. Hartinger, *Chem. Commun.* **2013**, *49*, 3348–3350; d) A. Grau-Campistany, A. Massaguer, D. Carrion-Salip, F. Barragán, G. Artigas, P. López-Senín, V. Moreno, V. Marchán, *Mol. Pharm.* **2013**, *10*, 1964–1976; e) M. Gobec, J. Kljun, I. Sosic, I. Mlinaric-Rascan, M. Ursic, S. Gobec I. Turel, *Dalton Trans.* **2014**, *43*, 9045–9051; f) R. Hudej, J. Kljun, W. Kandioller, U. Repnik, B. Turk, C. G. Hartinger, B. K. Keppler, D. Miklavčič, I. Turel, *Organometallics* **2012**, *31*, 5867–5874; g) L. He, S.-Y. Liao, C.-P. Tan, R.-R. Ye, Y.-W. Xu, M. Zhao, L.-N. Ji, Z.-W. Mao, *Chem. Eur. J.* **2013**, *19*, 12152–12160; h) F. Caruso, M. Rossi, A. Benson, C. Opazo, D. Freedman, E. Monti, M. B. Gariboldi, J. Shaulky, F. Marchetti, R. Pettinari, C. Pettinari, *J. Med. Chem.* **2011**, *55*, 1072–1081.
[13] a) N. P. E. Barry, F. Edafe, B. Therrien, *Dalton Trans.* **2011**, *40*, 7172–7180; b) N. P. E. Barry, O. Zava, J. Furrer, P. J. Dyson, B. Therrien, *Dalton Trans.* **2010**, *39*, 5272–5277; c) A. Mishra, H. Jung, J. W. Park, H. K. Kim, H. Kim, P. J. Stang, K.-W. Chi, *Organometallics* **2012**, *31*, 3519–3526; d) V. Vajpayee, S. m. Lee, J. W. Park, A. Dubey, H. Kim, T. R. Cook, P. J. Stang, K.-W. Chi, *Organometallics* **2013**, *32*, 1563–1566; e) A. Mishra, S. C. Kang, K.-W. Chi, *Eur. J. Inorg. Chem.* **2013**, 5222–5232.
[14] a) A. Bergamo, G. Sava, *Dalton Trans.* **2011**, *40*, 7817–7823; b) A. Levina, A. Mitra, P. A. Lay, *Metallomics* **2009**, *1*, 458–470; c) F. Wang, A. Habtemariam, E. P. L. van der Geer, R. Fernández, M. Melchart, R. J. Deeth, R. Aird, S. Guichard, F. P. A. Fabbiani, P. Lozano-Casal, I. D. H. Oswald, D. I. Jodrell, S. Parsons, P. J. Sadler, *Proc. Natl. Acad. Sci. USA* **2005**, *102*, 18269–18274; d) C. G. Hartinger, N. Metzler-Nolte, P. J. Dyson, *Organometallics* **2012**, *31*, 5677–5685; e) Y. K. Yan, M. Melchart, A. Habtemariam, P. J. Sadler, *Chem. Commun.* **2005**, 4764–4776.
[15] S. M. Meier, M. Hanif, Z. Adhireksan, V. Pichler, M. Novak, E. Jirkovsky, M. A. Jakupec, V. B. Arion, C. A. Davey, B. K. Keppler, C. G. Hartinger, *Chem. Sci.* **2013**, *4*, 1837–1846.
[16] F. Saleem, G. K. Rao, A. Kumar, G. Mukherjee, A. K. Singh, *Organometallics* **2013**, *32*, 3595–3603.
[17] a) R. Mitra, in: *Targeted Delivery of Cytotoxic Metal Complexes into Cancer Cells with and without Macromolecular Vehicles*, PhD Thesis, IISc, Bangalore, **2014**; b) R. Mitra, A. G. Samuelson, *RSC Adv.* **2014**, *4*, 24304–24306.
[18] N. J. M. Sanghamitra, M. K. Adwankar, A. S. Juvekar, V. Khurajjam, C. Wycliff, A. G. Samuelson, *Ind. J. Chem.* **2011**, *50A*, 465–473.
[19] M. A. Bennett, T. N. Huang, T. W. Matheson, A. K. Smith, S. Ittel, W. Nickerson, *16. (η^6-Hexamethylbenzene)Ruthenium Complexes*, in: *Inorganic Syntheses* (Ed.: J. P. Fackler), vol. 21, John Wiley & Sons, Inc., Hoboken **2007**, p. 74–78 (DOI: 10.1002/9780470132524.ch16).
[20] D. D. Perrin, W. L. F. Armarego, *Purification of Laboratory Chemicals*, Pergamon Press, Oxford, UK, **1988**.

[21] L. Farrugia, *J. Appl. Crystallogr.* **1999**, *32*, 837–838.
[22] G. M. Sheldrick, *SHELX-97* (release 97–2), University of Göttingen, Germany, **1997**.
[23] L. Farrugia, *J. Appl. Crystallogr.* **1997**, *30*, 565.
[24] a) J. Iwasa, T. Fujita, C. Hansch, *J. Med. Chem.* **1965**, *8*, 150–153; b) A. Noble, *J. Chromatogr. A* **1993**, *642*, 3–14; c) A. Paschke, P. L. Neitzel, W. Walther, G. Schüürmann, *J. Chem. Eng. Data* **2004**, *49*, 1639–1642.
[25] T. Lehóczki, É. Józsa, K. Ősz, *J. Photochem. Photobiol. A: Chem.* **2013**, *251*, 63–68.

Received: June 18, 2014
Published Online: October 14, 2014

